Revisiting magnetic exchange couplings in heterodinuclear complexes through the decomposition method in KS-DFT

Gwenhaël Duplaix-Rata, Boris Le Guennic, Gregoire David

Revisiting magnetic exchange couplings in heterodinuclear complexes through the decomposition method in KS-DFT

Gwenhaël Duplaix-Rata, Boris Le Guennic, and Grégoire David*

Univ Rennes, CNRS, ISCR (Institut des Sciences Chimiques de Rennes)-UMR 6226, F-35000 Rennes, France

E-mail: gregoire.david@univ-rennes1.fr

Abstract

Providing tools to understand the physical mechanisms governing magnetic properties in transition metal-based compounds is still of great interest. Here, the magnetic exchange coupling in a series of heterodinuclear complexes is investigated by means of the *decomposition* method. This work presents the first application of the *decomposition* method to systems where magnetic centres may bear more than one unpaired electron. By decomposing the coupling into three physical contributions (direct exchange, kinetic exchange, and spin polarisation), we provide numerical arguments to confirm or infirm the rationalisation allowed by the conceptual analysis of the magnetic d orbitals. We also take advantage of the recently proposed generalisation of the method [David *et al., J. Chem. Theory Comput.*, 2023, **19**, 157] to get more insights into the underlying mechanisms by disentangling the coupling between centres into its electron-electron interactions.

1 Introduction

Magnetic exchange coupling J is a fundamental property resulting from the interaction between at least two unpaired electrons localised on different magnetic centres. Favouring the parallel (ferromagnetic coupling) or antiparallel (antiferromagnetic coupling) alignment of electrons, it may play a critical role in the design of molecules with predefined magnetic properties.[1] However, magnetic interactions are often very complicated to rationalise and in this context, theoretical and computational chemistry have provided essential insights in proposing either numerically accurate determination or conceptual interpretation of properties.[2,3] In theoretical chemistry, the determination of J is mostly based on the energy difference between the high spin (HS) state and a lower spin state. Hence, a proper and consistent description of both states is fundamental.

Theoretical treatment of magnetic systems requires highly sophisticated approaches in order to properly describe the multi-configurational character of the wave-function.[2] In this context, wave-function-based methods are the reference approaches where the static correlation is taken into account mostly with CASSCF-type of calculations.[4,5] Moreover, the dynamical correlation effects may be critical too, being more often accounted on-top of a CASSCF calculation through perturbation theory (CASPT2[6–8] or NEVPT2) or Configuration Interaction[9] (CI). For computing magnetic exchange couplings, this last strategy provided the most adapted strategy with the Difference Dedicated CI method.[10] These methods provide very accurate evaluations of small vertical energy differences as J. They may also be greatly instructive thanks to the effective Hamiltonian theory and the quasi-degenerate perturbation theory,[11–14] allowing to extract information from these complicated calculations and wave-functions.[3] However, in addition to certain expertise required to perform these calculations, the computational cost of wave-function-based methods is most of the time prohibitive for *real life* applications.

On the contrary, Kohn-Sham density functional theory[15,16] (KS-DFT) has probably become the most widely used approach in quantum chemistry by dint of its ability to describe

correlation effects at the mean-field level. Despite this success, KS-DFT is based on the description through one Slater determinant and fails to properly describe magnetic systems. Indeed, open-shell low-spin states must be described by several configurations to properly satisfy the spin and spatial symmetry requirements of the wave-function. Hence, whilst the former may fairly be described in KS-DFT, the latter usually resorts to the use of a broken symmetry (BS) determinant, where the low spin state is approximated by only one configuration.[17,18] The BS determinant being not an eigenfunction of $\hat{S}^2$, i.e. a pure spin state, the energy difference between both determinants must be *spin decontaminated* and in this framework, the use of the Yamaguchi formula is certainly the most common spin decontamination scheme.[17–26] Other approaches have been proposed in DFT to overcome the use of a BS determinant such as based on the spin-flip,[27–32] non-collinear,[33,34] fractionally-occupied[35–38] and multireference approaches[39–41] or constrained DFT..[42,43] Despite this, the BS strategy has been widely used to compute magnetic exchange coupling over the last decades, providing a valuable semi-quantitative evaluation of J in various compounds.[2,44,45]

From the work of de Loth *et al.*[46] and Calzado *et al.*[11–13] using the quasi-degenerate perturbation theory, the magnetic exchange coupling may be rationalised as the competition between several physical contributions; the reader should refer to Ref. 11 for a deeper discussion in the wave-function theory framework. Among them, the three main competing contributions are i) the direct exchange between both magnetic centres, ii) the anti-ferromagnetic kinetic exchange contribution analogue to the Anderson superexchange contribution and iii) the spin polarisation contribution, caused by the differential response of the non-magnetic orbitals to the different fields created by the unpaired electrons in the HS and low spin states.[2,11] Whilst BS KS-DFT was supposed to provide only a numerical evaluation of J, Ferré *et al.* proposed the *decomposition* scheme based on selective relaxations of the orbitals involved in the different mechanisms to extract these contributions.[47,48] Initially developed as a rationalisation tool, this method allowed getting insights into various situations such as investigating J in dinuclear copper complexes,[49] parametrising model Hamiltonians of

a quantum spin liquid[50] or analysing the symmetry breaking in disjoint diradicals.[51] More recently, some of the present authors took advantage of the *decomposition* scheme to propose a new paradigm to compute the magnetic exchange coupling in two magnetic centres systems,[52] overcoming some pathological consequences from the use of the traditional spin-decontamination technique.[53] Indeed, evaluating J by taking the sum of the three properly extracted and spin-decontaminated contributions provides a more consistent determination than through the Yamaguchi formula where the non-adapted treatment of the spin polarisation effects may result in strong over- or underestimation of couplings.[52,54] This strategy has very recently been generalised to any number of magnetic centres. It offers a new affordable route to compute properly spin-decontaminated magnetic exchange couplings in systems featuring more than two magnetic centres, a situation where the spin contamination is almost all the time neglected.[55] However, to date, the *decomposition* scheme has only been limited to couplings involving one unpaired electron per magnetic centre.

This work presents the extension and first applications of the *decomposition* scheme to dinuclear systems featuring more than one electron per magnetic centre. To stress the method out, its application focuses on a series of heterodinuclear Cu(II)-M complexes (with M = Cr(III), Mn(III), Mn(II), Fe(III), Co(II), Ni(II) and Cu(II)), keeping a Cu(II) magnetic centre with only one unpaired electron.[56] This paper is organised as follows. Section 2 presents the extraction of the different contributions in the context of two magnetic centres, of which one of them bears several unpaired electrons. It follows the description of compounds studied in section 3 and the computational details in section 4. Finally, section 5 discusses the decomposition of the magnetic exchange coupling of the 8 systems in line with the orbital analysis.

2 General decomposition of J in systems with two magnetic centres

The magnetic exchange interaction between two magnetic centres A and B is usually described by the Heisenberg-Dirac-van Vleck Hamiltonian,

$$\hat{H}^{\mathrm{HDvV}} = -2J\hat{S_A} \cdot \hat{S_B} \tag{1}$$

where J expresses the magnitude of the coupling between both magnetic centres with which the *local* spin operators $\hat{S_A}$ and $\hat{S_B}$ are associated. In the context of the present work, the magnetic centres may bear several unpaired electrons and are considered as local high spin states according to the HDvV Hamiltonian, i.e. the spin of all unpaired electrons on a site are parallelly aligned.

Let us take the example of a system featuring two magnetic centres, A and B, bearing n_A and 1 unpaired electrons, respectively. The decomposition of the magnetic exchange coupling starts with the computation of the high spin $S = (n_A+1)/2$ state in the restricted open-shell formalism (RO). Once the $n_A + 1$ singly occupied molecular orbitals (MOs) localised, this determinant may be expressed as,

$$\Phi_{\mathrm{HS,RO}} = \Phi_{AB,\mathrm{RO}} = |\prod_{i}^{n_c} i\bar{i} \prod_{\alpha}^{n_A} a_\alpha b| \tag{2}$$

with i the n_c core (non-magnetic) doubly occupied orbitals, a_α the n_A magnetic orbitals associated to the centre A and b the magnetic orbital associated to the centre B. Flipping the spin of all electrons of one magnetic centre, without optimising any orbital, allows one to generate a first BS determinant,

$$\Phi_{\mathrm{BS,NO}} = \Phi_{A\bar{B},\mathrm{NO}} = |\prod_{i}^{n_c} i\bar{i} \prod_{\alpha}^{n_A} a_\alpha \bar{b}| \tag{3}$$

where NO stands for non-optimised. Using the energies of these two first determinants in addition to the Yamaguchi formula, one may extract the direct exchange contribution as,

$$J_0 = \frac{E[\Phi_{A\bar{B},\mathrm{NO}}] - E[\Phi_{AB,\mathrm{RO}}]}{\langle \hat{S}^2 \rangle_{\Phi_{AB,\mathrm{RO}}} - \langle \hat{S}^2 \rangle_{\Phi_{A\bar{B},\mathrm{NO}}}} \tag{4}$$

It may be worth noting that the spin decontamination factor has here the same effect as S in the spin pure energy difference derived from Eq. (1),

$$J = \frac{E(S-1) - E(S)}{2S} \tag{5}$$

with S the spin quantum number of the HS state.

The second step consists in extracting the kinetic exchange contribution by relaxing the magnetic orbitals obtained at the HS,RO stage. This is done through a selective relaxation of these involved orbitals while keeping the core orbitals frozen, resulting in a new BS determinant such as,

$$\Phi_{A'\bar{B}',\mathrm{FC}} = |\prod_{i}^{n_c} i\bar{i} \prod_{\alpha}^{n_A} a'_\alpha \bar{b}'| \tag{6}$$

where FC stands for frozen core and the prime symbolises the relaxed orbitals. Using the energy and the $\langle \hat{S}^2 \rangle$ of this determinant in addition to the previous results, one may evaluate the kinetic exchange contribution as,

$$\Delta J_{KE} = \frac{E[\Phi_{A'\bar{B}',\mathrm{FC}}] - E[\Phi_{AB,\mathrm{RO}}]}{\langle \hat{S}^2 \rangle_{\Phi_{AB,\mathrm{RO}}} - \langle \hat{S}^2 \rangle_{\Phi_{A'\bar{B}',\mathrm{FC}}}} - J_0 \tag{7}$$

Finally, the last contribution, corresponding to the spin polarisation effects, is obtained by relaxing the core orbitals of both HS,RO and BS,NO determinants while keeping their magnetic orbitals frozen. It results in two new determinants,

$$\Phi_{AB,\mathrm{FM}} = |\prod_{i}^{n_c} i'\bar{i}' \prod_{\alpha}^{n_A} a_\alpha b| \tag{8}$$

for the HS and,

$$\Phi_{A\bar{B},\mathrm{FM}} = |\prod_{i}^{n_c} i'\bar{i}' \prod_{\alpha}^{n_A} a_\alpha \bar{b}| \tag{9}$$

for the BS, where FM stands for frozen magnetic orbitals, the contribution may be then extracted as,

$$\Delta J_{SP} = \frac{E[\Phi_{A\bar{B},\mathrm{FM}}] - E[\Phi_{AB,\mathrm{FM}}]}{\langle \hat{S}^2 \rangle_{\Phi_{AB,\mathrm{RO}}} - \langle \hat{S}^2 \rangle_{\Phi_{A\bar{B},\mathrm{NO}}}} - J_0 \tag{10}$$

The overall magnetic exchange coupling may be evaluated through the *recomposition* method by taking the sum of these three contributions as[52,55]

$$J_\Sigma = J_0 + \Delta J_{\mathrm{KE}} + \Delta J_{\mathrm{SP}}. \tag{11}$$

3 Molecular models

The presence of several unpaired electrons per magnetic centre may result in more subtle magnetic interactions than the magnetic exchange coupling, such as the biquadratic exchange occurring between two $S = 1$ magnetic centres.[2] To restrict the present work to the study of J only, we consider a series of heteronuclear Cu(II)-M complexes with M = Cr(III), Mn(III), Mn(II), Fe(III), Co(II), Ni(II) and Cu(II), and labelled (**1**), (**2**), (**3**), (**4**)/(**4a**), (**5a**), (**7a**) and (**8**), respectively, according to Ref 56 and presented in Table 1. All structures consist in a Cu(II) centre encapsulated in a 3,9-dimethyl-4,8-diazaundeca-3,8-diene-2,10-dione dioxime (Dopn) oximato-bridged to the M centre, capped in a tridentate cyclic amine 1,4,7-trimetyl-1,4,7-triazacyclononane (L). Furthermore, (**2**), (**3**), (**4a**), (**5a**) and (**7a**) present another bridging ligand with a carboxylato group. Only the crystal and molecular structures of (**1**) and (**2**), referred to as HEWMAX and HEWMEB in the Cambridge Structural Database[57] (CSD), respectively, have been established by X-ray diffraction. Hence, after having validated the relevance of the optimised geometries with (**1**) and (**2**), the optimised structures of all compounds have been used and are presented in Fig. 1.

All couplings of the present series of complexes have been experimentally determined

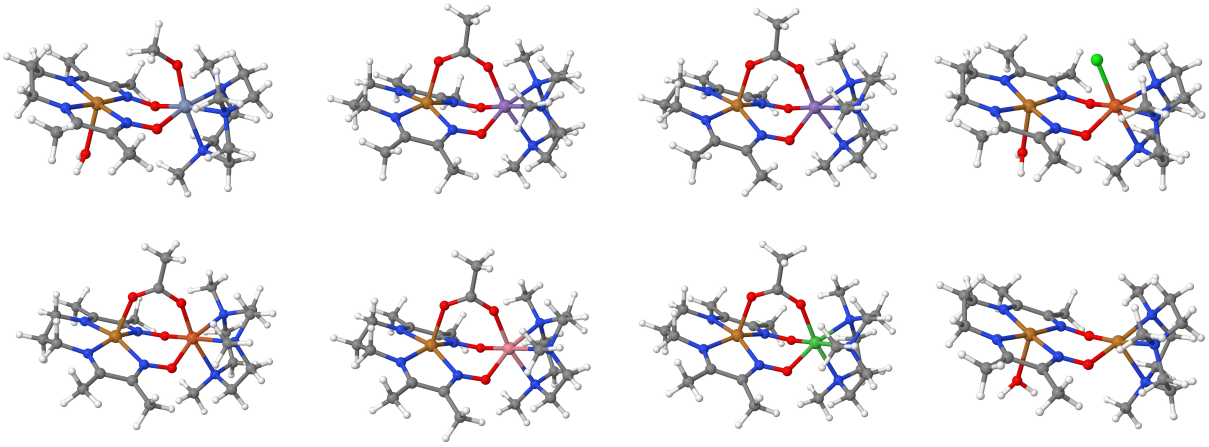

Figure 1: Optimised molecular structure of all Cu(II)-M complexes studied with (**1**), (**2**), (**3**), (**4**) from the left to the right of the first row and (**4a**), (**5a**), (**7a**) and (**8**) from the left to the right of the second row. Brown = copper, blue slate = chromium, purple = manganese, bronze = iron, pink slate = cobalt, dark green = Ni, blue = nitrogen, red = oxygen, grey = carbon, white = hydrogen, green = chlorine.

through magnetic susceptibility measurements and are presented in Table 1. They go from a weak ferromagnetic coupling for (**1**) at +19 cm to a strongly antiferromagnetic one at -298 cm^{-1} for (**8**), covering a large scope of different couplings. These values may be readily rationalised through orbital analysis[56] and this set of molecules offers then a great opportunity to stress the method out on some well-known examples whilst providing some numerical trend to this rationalisation.

Finally, it may be worth noting that computing the coupling of (**1**) and (**2**) has been used several times to test KS-DFT based methods.[42,43,58–60]

Table 1: Formula, electronic configuration of the M centre and experimental magnetic exchange coupling in cm^{-1} of the M-Cu(II) complexes.

	Complex	M	Conf.	J_{exp}
(**1**)	$[(Dopn)Cu^{II}(OH_2)Cr^{III}(OCH_3)L]^-$	Cr^{III}	d^3	+19
(**2**)	$[(Dopn)Cu^{II}(\mu\text{-}OOCH_3)Mn^{III}L]^{2-}$	Mn^{III}	d^4	+54
(**3**)	$[(Dopn)Cu^{II}(\mu\text{-}OOCH_3)Mn^{II}L]^-$	Mn^{II}	d^5	-41
(**4**)	$[(Dopn)Cu^{II}(OH_2)Fe^{III}(Cl)L]^-$	Fe^{III}	d^5	-39
(**4a**)	$[(Dopn)Cu^{II}(\mu\text{-}OOCH_3)Fe^{III}L]^{2-}$	Fe^{III}	d^5	-45
(**5a**)	$[(Dopn)Cu^{II}(\mu\text{-}OOCH_3)Co^{II}L]^-$	Co^{II}	d^7	-54
(**7a**)	$[(Dopn)Cu^{II}(\mu\text{-}OOCH_3)Ni^{II}L]^-$	Ni^{II}	d^8	-99
(**8**)	$[(Dopn)Cu^{II}(OH_2)Cu^{II}(OH_2)L]^{2-}$	Cu^{II}	d^9	-298

4 Computational details

Among the eight studied complexes, only the structure of (**1**) and (**2**) have been experimentally determined. The first part of this work consists in comparing the experimental crystallographic structure, where the hydrogen atoms have been optimised, with the fully optimised (**1**) and (**2**) structures. Once the relevance of the all-atom optimised geometries is validated for (**1**) and (**2**), the other compounds has been optimised and used throughout this work. All optimisations have been performed with Orca[61] using the B3LYP functional[62–65] and the def2-SVP basis set for all atoms except the transition metal ones, of which the def2-QZVPP[66] basis set have been employed.

The decomposition and computation of magnetic exchange couplings have been carried out using the PBE0 functional[67–69] with 30% of Hartree-Fock exchange whilst the same combination of basis sets used for the geometry optimisations has been employed. The amount of HF exchange is a key quantity when transition metal-based compounds are studied and a balance of 30 to 35% has been several times advised.[70,71] In this regard, PBE0 being only built with two HF and GGA exchange functionals provides an unambiguous definition of this mixing; for instance, compared to the very popular three parameters B3LYP functional (where LDA exchange is also considered). The selective relaxation of the orbitals has been done using the LSCF method[72] present in Orca since version 4.2.0.[61] All molecular structures have been visualised using Jmol.[73] Supplementary information gives all structures used in this work and the details of all calculations (energies and expectation values of $\hat{S}^2$).

Table 2 presents the comparison between the experimentally and theoretically determined magnetic exchange couplings as well as a comparison of the structural parameters for (**1**) and (**2**) using the crystallographic structure and the fully optimised geometry. The couplings of both compounds (**1**) and (**2**) have been experimentally determined as ferromagnetic at 19 and 54 cm^{-1}, respectively.[56] Using the crystallographic structure, the DFT determination using the Yamguchi formula correctly represents the sign and the magnitude of the coupling of both (**1**) and (**2**) compounds, with a very slight underestimation ($J_{\text{Yamaguchi}} = 11$ cm^{-1})

Table 2: Experimental J value (J_{exp}) and J from the usual use of the Yamaguchi formula ($J_{\text{Yamaguchi}}$) in cm^{-1} and details of the structural parameters ($\angle$N-Cu-N (°), $\angle$O-M-O (°), $d_{\text{Cu-M}}$ (Å) and $\theta_{\text{Cu-N-O-M}}$ (°)) of the X-ray and optimised geometries for (**1**) et (**2**).

	(**1**) Cu(II)-Cr(III) $d^9 - d^3$		(**2**) Cu(II)-Mn(III) $d^9 - d^4$	
	X-ray	opt	X-ray	opt
J_{exp}	19		54	
$J_{\text{Yamaguchi}}$	11	23	54	94
$\angle$N-Cu-N (°)	97.1	100.0	98.2	96.4
$\angle$O-M-O (°)	100.9	95.0	97.1	95.7
$d_{\text{Cu-M}}$ (Å)	3.86	3.77	3.54	3.57
$\theta_{\text{Cu-N-O-M}}$ (°)	-32.2	-39.4	26.8	20.3

and a good agreement ($J_{\text{Yamaguchi}} = 54$ cm^{-1}), respectively. The computation of J from the fully optimised structure yields stronger couplings with a slight overestimation for (**1**) with $J_{\text{Yamaguchi}} = 23$ cm^{-1} and a larger difference for (**2**) with $J_{\text{Yamaguchi}} = 94$ cm^{-1}. These differences in the computed values of J may readily be related to the changes in the structural parameters in the geometry optimisation. Indeed, even small changes of the ligand-metal-ligand angles or the metal-metal distances may have a relative strong impact on J and these dependances of J on the structure have been highlighted at the early stage of the molecular magnetism.[74] Nevertheless, the computation of J on the optimised structures are consistent and ensure the relevance of their use throughout this work.

5 Results and discussions

Table 3 presents the experimental determination and both $J_{\text{Yamaguchi}}$ and J_{Σ} theoretical evaluations of J as well as the decomposition for all heteronuclear compounds. First of all, both DFT evaluations provide very close results whilst they agree with the experimental values for the whole series.

Table 3: Experimental J value (J_{exp}) and J from the usual use of the Yamaguchi formula ($J_{\text{Yamaguchi}}$), *recomposition* (J_{Σ}) and decomposition (J_0, ΔJ_{KE} and ΔJ_{SP}) obtained for all compounds in their optimised geometries in cm^{-1}.

Cu(II)-M	(**1**) Cr(III) d^3	(**2**) Mn(III) d^4	(**3**) Mn(II) d^5	(**4**) Fe(III) d^5	(**4a**) Fe(III) d^5	(**5a**) Co(II) d^7	(**7a**) Ni(II) d^8	(**8**) Cu(II) d^9
J_{exp}	19	54	-41	-39	-45	-54	-99	-298
$J_{\text{Yamaguchi}}$	23	94	-37	-29	-48	-60	-93	-275
J_{Σ}	28	121	-31	-23	-41	-52	-83	-240
J_0	26	63	16	39	35	27	45	131
ΔJ_{KE}	-1	-2	-45	-55	-77	-79	-131	-388
ΔJ_{SP}	2	60	-2	-7	1	-1	3	18

5.1 Decomposition in the (5a), (7a) and (8) complexes

Let us now focus on the decomposition by considering the simplest case of the Cu(II)-Cu(II(II)) compound (**8**). Both copper atoms are coordinated in a square pyramidal arrangement, yielding two singly occupied $d_{x^2-y^2}$-*like* orbitals of which the lobes point towards the ligands as presented in Fig. 2. As expected and already discussed by Birkelbach *et al.*,[56] this situation results in an important direct exchange contribution and a stronger kinetic exchange contribution through a σ exchange pathway. This is numerically confirmed by the decomposition where the ferromagnetic J_0 is equal to 131 cm^{-1} and ΔJ_{KE} is almost three times larger at -388 cm^{-1}, resulting in an overall strong antiferromagnetic coupling. As expected for couplings between transition metals, the spin polarisation contribution is here negligible compared to the magnitude of the other terms. Taking now a step to the left in the periodic table, compound (**7a**) corresponds to a situation where M bears two unpaired

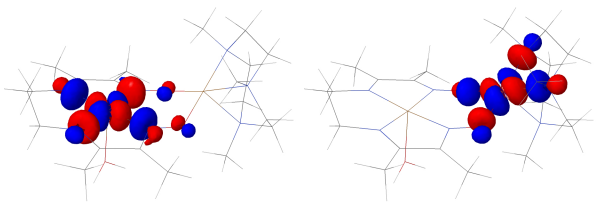

Figure 2: Localised magnetic orbitals obtained from the $\Phi_{\text{HS,RO}}$ determinant for (**8**). Isovalue = 0.05 a.u..

electrons occupying a d_{z^2} and $d_{x^2-y^2}$-*like* orbitals due to the nearly octahedral environment of the Ni(II) ion (Fig. 3). This new interaction between the $d_{x^2-y^2}$ orbital of the Cu(II) and the d_{z^2} orbital of the Ni(II) mainly results in a ferromagnetic contribution due to the orientation of the latter. However, the drastic reduction in the magnitude of the coupling between (**8**) and (**7a**), going experimentally from -298 to -99 cm^{-1}, respectively, cannot be attributed to this additional ferromagnetic contribution only. Indeed, the decomposition shows an important decrease in the strength of both J_0 and ΔJ_{KE} contributions, whilst the latter is still dominating. Similar conclusions may be drawn by looking at the Cu(II)-Co(II) complex (**5a**). Indeed, the d^7 configuration corresponds to 3 unpaired electrons where an additional t_{2g}-*like* orbital is occupied as shown in Fig. 4. This new interaction with the $d_{x^2-y^2}$ orbital of the Cu(II) does not provide a new pathway for the kinetic exchange but should correspond to a new ferromagnetic J_0 contribution. Hence, it results in an even weaker antiferromagnetic coupling experimentally evaluated at -54 cm^{-1} and as for (**7a**), the strength of all contributions is smaller with a dominating ΔJ_{KE} at -79 cm^{-1} and J_0 at 27 cm^{-1}.

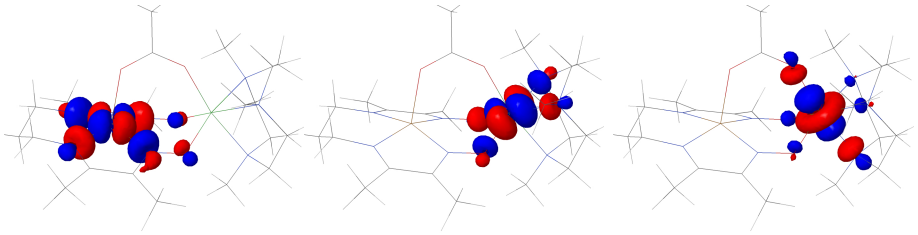

Figure 3: Localised magnetic orbitals obtained from the $\Phi_{HS,RO}$ determinant for (**7a**). Isovalue = 0.05 a.u..

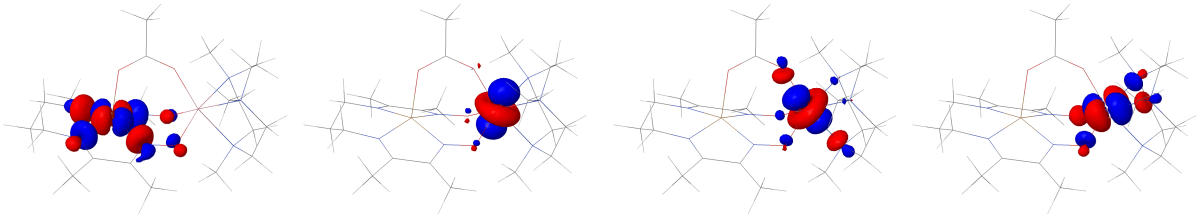

Figure 4: Localised magnetic orbitals obtained from the $\Phi_{HS,RO}$ determinant for (**5a**). Isovalue = 0.05 a.u..

Let us now take the *decomposition* scheme a step further to get more insights into the couplings of the (**5a**), (**7a**) and (**8**) compounds and to investigate the effect of the presence of more unpaired electrons. Some of the present authors recently generalised the *decomposition* scheme to the context of systems featuring several couplings with one unpaired electron per magnetic centre.[55] We use this strategy here to provide a thinner description of the coupling in extracting the individual electron-electron interactions, considering each magnetic orbital as a site. This allows us to decompose these different electron-electron interactions into their direct and kinetic exchange contributions presented in Table 4.

Let us start with the first part of Table 4 by considering the J_0 contribution from the interaction between the $d_{x^2-y^2}$ orbital of the Cu(II) and the different singly occupied magnetic orbitals of the M centre in (**5a**), (**7a**) and (**8**), their sum and the overall J_0; which differs from the sum by the application of the spin decontamination factor. For compound (**8**) the M centre only bears one unpaired and the $d_{x^2-y^2}$-$d_{x^2-y^2}$ interaction obviously concentrates all the interaction with a direct exchange contribution at 131 cm^{-1}. Going now to (**7a**), the direct exchange contribution coming from the $d_{x^2-y^2}$-$d_{x^2-y^2}$ interaction drastically decreases with strength at 75 cm^{-1} compared to (**8**). The new interaction occurring with the singly occupied d_{z^2} orbital on the Ni(II) centre yields a weak direct exchange contribution at 15 cm^{-1}. Both results in an overall sum much weaker than for (**8**) at 90 cm^{-1}, whilst the direct exchange contribution to the coupling is finally 45 cm^{-1}. In (**5a**), the contribution coming from the interaction between the $d_{x^2-y^2}$ orbitals and between the $d_{x^2-y^2}$ and the d_{z^2} orbitals are of the same magnitude but slightly smaller, at 62 and 12 cm^{-1}, respectively. The $d_{x^2-y^2}$-t_{2g} interaction provides a very weak contribution at 7 cm^{-1}. Finally, the sum is of the same order of magnitude as for (**7a**) at 81 cm^{-1} but results in a small direct exchange contribution at 27 cm^{-1}.

The right part of Table 4 shows the contribution to the kinetic exchange of the interactions between the $d_{x^2-y^2}$ orbital of the Cu(II) and the different singly occupied magnetic orbitals of the M centre in (**5a**), (**7a**) and (**8**), their sum and the overall ΔJ_{KE}. As for the

Table 4: Individual contribution from each d^{Cu}-d^{M} interaction, their sum and the final contribution to the magnetic exchange coupling for the direct and kinetic exchange terms of (**5a**), (**7a**) and (**8**) in cm^{-1}. The sum and the final contribution to the coupling differ by the application of the spin decontamination factor in the latter.

d^{Cu}	d^{M}		(**5a**) Co(II)	(**7a**) Ni(II)	(**8**) Cu(II)		(**5a**) Co(II)	(**7a**) Ni(II)	(**8**) Cu(II)
	$d_{x^2-y^2}$		62	75	131		-239	-263	-395
$d_{x^2-y^2}$	d_{z^2}	$J_0^{d\text{-}d}$	12	15		$-2t^2/U$	0	None	
	t_{2g}		7				None		
		$\sum J_0^{d\text{-}d}$	81	90	131	$\sum -2t^2/U$	-239	-263	-395
		J_0	27	45	131	ΔJ_{KE}	-79	-131	-388

direct exchange, the last two differ by the application of the spin decontamination factor. In addition, while ΔJ_{KE} is calculated from Eq (7), the sum comes from the use of the Hubbard Hamiltonian parameters t and U and both evaluations may slightly differ.[52] This explains the tiny difference for (**8**) between $\sum -2t^2/U = -395$ cm^{-1} and $\Delta J_{KE} = -388$ cm^{-1}. For the complex (**7a**), there is a critical decrease in the magnitude of the kinetic exchange contribution coming from the interaction between the $d_{x^2-y^2}$ orbitals, with a contribution 1.5 times smaller at -263 cm^{-1}. Furthermore, the interaction between the electron occupying the $d_{x^2-y^2}$ of the Cu(II) and the d_{z^2} of the Ni(II) does not provide any contribution and is labelled as "None" since absolutely no relaxation effects occur. The final kinetic exchange contribution for (**7a**) is equal to -131 cm^{-1} and entirely comes from the $d_{x^2-y^2}$-$d_{x^2-y^2}$ interaction. Finally, for the complex (**5a**), the observations are in line with the remarks drawn for the direct exchange. The $d_{x^2-y^2}$-$d_{x^2-y^2}$ interaction contributes to the kinetic exchange with a magnitude similar to (**7a**) at -239 cm^{-1}. For the $d_{x^2-y^2}$-d_{z^2} interaction, tiny relaxations occur but yield negligible contribution, below the cm^{-1}, whilst nothing happens between the $d_{x^2-y^2}$-t_{2g} orbitals. Finally, the kinetic exchange entirely comes from the interaction between the $d_{x^2-y^2}$ orbitals and results in a kinetic exchange contribution to the overall coupling at -79 cm^{-1}.

5.2 Decomposition in the (3), (4) and (4a) complexes

The series of hetereodinuclear compounds is constituted of three complexes with a d^5 M ion, (**4**) and (**4a**) featuring Fe(III) ions and (**3**) an Mn(II) ion. All of them present rather similar couplings experimentally at -41, -39 and -45 cm^{-1} for (**3**), (**4**) and (**4a**), respectively. However, the difference between the couplings of the three compounds is more marked theoretically, with J_Σ at -31, -23 and -41 cm^{-1} for (**3**), (**4**) and (**4a**), respectively. Comparing the Fe(III) complexes (**4**) and (**4a**), both couplings present similar direct exchange contributions at 39 and 35 cm^{-1}, respectively. Hence, the difference in the overall couplings results from different ΔJ_{KE}, at -55 cm^{-1} for (**4**) and -77 cm^{-1} for (**4a**). Both compounds differ in the presence of an additional carboxylato bridging ligand between both metal ions in (**4a**). In addition to a possible new pathway for the kinetic exchange, it induces strong structural changes such as the dihedral $\theta_{\text{Cu-N-O-M}}$ angle which is equal to 40 ° in (**4**) and 20 ° in (**4a**). The last compound of the d^5 series features an Mn(II) metal centre, with a coupling of strength between both Fe(III) complexes at -31 cm^{-1} for J_Σ. However, this compound presents a different decomposition. Indeed, in complex (**3**) a weaker direct exchange contribution at 16 cm^{-1} occurs, which can be related to the shape of the d orbitals. Shown Fig. 5, the $d_{x^2-y^2}$-*like* orbital of the Mn(II) centre of (**3**) appears less diffused than the same orbital on the Fe(III) centre in (**4a**) and would result in a weaker J_0 contribution. In line with J_0, the kinetic exchange contribution is smaller than in (**4**) or (**4a**), but the competition between both contributions yields a coupling of the same magnitude.

5.3 Decomposition in the (1) and (2) complexes

Finally, the discussion ends with the two last compounds (**1**) and (**2**), the only complexes of the series exhibiting a ferromagnetic coupling. Indeed, according to the decomposition the kinetic exchange contribution in both compounds is almost null whilst the J_0 contribution is important (Table 3). This coincides with the d^3 and d^4 configurations of the M ion in (**1**) and (**2**), respectively: since the $d_{x^2-y^2}$-*like* of the M centre is empty, no kinetic exchange

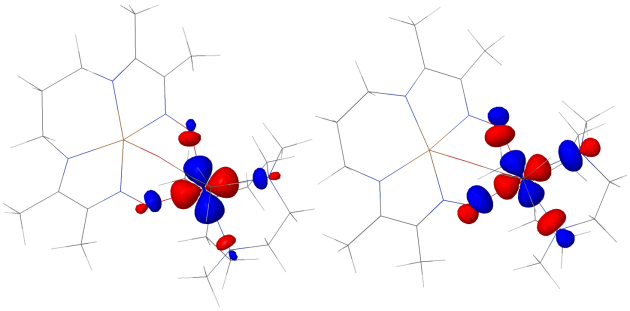

Figure 5: $d_{x^2-y^2}$-*like* localised magnetic orbital of the M centre obtained from the $\Phi_{\mathrm{HS,RO}}$ determinant for the complexes (**3**) (M=Mn(II), left) and (**4a**) (M=Fe(III), right). Isovalue = 0.05 a.u..

mechanism may occur. However, whilst compound (**1**) shows a rather expected coupling and decomposition according to the previous discussions, compound (**2**) is strongly ferromagnetic due to both strong ferromagnetic J_0 and ΔJ_{SP}.

Whilst according to an orbital analysis, complex (**2**) is well expected to exhibit a ferromagnetic coupling, the *decomposition* scheme sheds light on a different story. Indeed, in addition to a significantly strong direct exchange contribution at 63 cm^{-1}, the complex exhibits a strong ferromagnetic spin polarisation contribution at 60 cm^{-1} whilst this quantity is negligible for all other compounds of the series. Furthermore, both $J_{\mathrm{Yamaguchi}}$ and J_{Σ} evaluations show a rather large discrepancy for (**2**) compared to all other compounds.

The strong direct exchange contribution may be readily explained by plotting the $d_{x^2-y^2}$-*like* orbitals on the Cu(II) centre coming from the localisation of the SOMOs of the $\Phi_{\mathrm{HS,RO}}$ determinant. Fig. 6 shows these orbitals for complexes (**1**), (**2**) and (**3**). Whilst for (**1**) and (**3**) the orbitals look very well localised on the copper atom, this orbital exhibits a

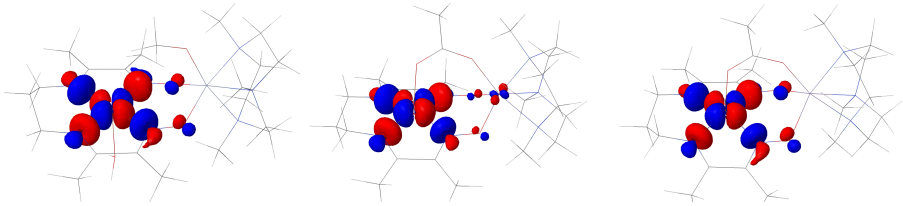

Figure 6: $d_{x^2-y^2}$-*like* localised magnetic orbital of the Cu centre obtained from the $\Phi_{\mathrm{HS,RO}}$ determinant for complexes (**1**) (M=Cr(III), top left), (**2**) (M=Mn(III), top right) and (**3**) (M=Mn(II), bottom). Isovalue = 0.05 a.u..

non-negligible delocalisation tail over the Mn centre for (**2**). Hence, one may easily think that this spreading over the other centre would result in a greater exchange term between this orbital and the orbitals localised on the Mn centre. This explains the extravagant spin polarisation contribution since this contribution directly results from the spin distribution of the magnetic electrons. As a reminder, the spin polarisation contribution results from the differential response of the core orbitals due to the different fields created by the unpaired electrons in the HS and BS situation. Let us take now the example of the BS determinant with a β electron populating the $d_{x^2-y^2}$ orbital of the Cu(II) ion. It may readily be thought that the delocalisation tail of this β electron over an α spin centre will reduce the spin density ($\rho_\alpha(r) - \rho_\beta(r)$) on this site. On a contrary, it will increase this spin density for the HS state and one can easily imagine why this situation results in a large spin polarisation contribution.

This delocalisation tail gives us a beginning of explanation to the discrepancy between $J_{\text{Yamaguchi}}$ and J_Σ as well. Indeed, whilst in the HS the electron on the Cu can slightly move to the empty Mn orbital, this situation would not be favourable in the BS determinant and one may imagine that a fully optimised, i.e. unrestricted, calculation would lead to a reorganisation of the electronic distribution. In the *decomposition*, one fixes the first situation by using the orbitals of the HS.RO determinant as a common description which results in exaggerated J_0 and ΔJ_{SP} contributions. However, the *decomposition* scheme relies on the HDvV Hamiltonian where one considers well-localised spin centres. Complex (**2**) slightly deviates from this model and, whilst fully optimised calculations can still deal with the situation, the decomposition is more sensitive to this deviation. This opens the way to future development for the treatment of mixed valence compounds. However, it is worth mentioning that even though the decomposition overestimates the J_0 and ΔJ_{SP} contributions, these terms are not an artefact of the decomposition. Indeed, both HS and BS unrestricted determinants present very large spin contamination of 0.097 and 0.084, respectively, translating the strong effects of spin polarisation (see SI).

6 Conclusion

In this work, we have presented the extension and the first application of the *decomposition* scheme of magnetic exchange coupling to systems featuring two magnetic centres, of which one may bear several unpaired electrons. Following the previous works of some of the authors, the extraction is based on successive calculations of high-spin and broken-symmetry determinants, with selective relaxations of the orbitals involved in the different mechanisms.

We applied the methodology to a series of heterodinuclear compounds based on a Cu-M pattern with M = Cr(III), Mn(III), Mn(II), Fe(III), Co(II), Ni(II) and Cu(II). This allowed to stress the method out on well-known complexes exhibiting different occupation and configuration of the magnetic d orbitals. This work has confirmed and even refined the orbital analysis usually done for these transition metal-based complexes by providing numerical evaluations of the different contributions. However, the *decomposition* scheme also shed light on the physical mechanism governing the magnetic coupling in the Cu-Mn(III) compound (**2**), impossible to guess with a sole orbital analysis. Indeed, unlike all others this coupling exhibits a strong direct exchange as well as an unexpectedly strong ferromagnetic spin polarisation contribution.

We have also taken the rationalisation a step further by decomposing the coupling into its electron-electron interaction, benefiting from the recent developments of some of the authors on the multicentre systems. This allowed us to discuss and disentangle the real impact of the presence of new singly occupied d orbitals on the M centre, properly quantifying the orbital analysis.

In addition to the rationalisation, the *decomposition* scheme allows us to compute magnetic exchange couplings as the sum of the three main contributions, following our previous works on this aspect to a very consistent evaluation of J. Whilst the present compounds do not require a thinner treatment than the use of the Yamaguchi formula, it may be the case for systems presenting very strong spin polarisation effects.[52–54]

Future works will focus on the computation and decomposition of magnetic exchange

couplings in systems with several coupling paths and where magnetic centres bear several unpaired electrons. Furthermore, this work opened the discussion on the treatment of mixed-valence compounds and future works will be dedicated to this task.

Acknowledgement

The authors thank the French GENCI/IDRIS-CINES centres for high-performance computing resources. G.D. is grateful to Jean-Paul Malrieu (LCPQ, Univ. Paul-Sabatier, Toulouse, France) and Nicolas Ferré (ICR, Univ. Aix-Marseille, Marseille, France) for all discussions over the last years. G.D. received research funding from the European Union's 843 Horizon 2020 Research and Program under Marie Skłodowska-Curie Grant Agreement No. 899546.

References

(1) Coronado, E. Molecular magnetism: from chemical design to spin control in molecules, materials and devices. *Nature Reviews Materials* **2019**, *5*, 87–104.

(2) Malrieu, J. P.; Caballol, R.; Calzado, C. J.; de Graaf, C.; Guihéry, N. Magnetic Interactions in Molecules and Highly Correlated Materials: Physical Content, Analytical Derivation, and Rigorous Extraction of Magnetic Hamiltonians. *Chemical Reviews* **2013**, *114*, 429–492.

(3) de Graaf, C.; Broer, R. *Magnetic Interactions in Molecules and Solids*; Springer International Publishing, 2015.

(4) Roos, B. O.; Taylor, P. R.; Siegbahn, P. E. A complete active space SCF method (CASSCF) using a density matrix formulated super-CI approach. *Chemical Physics* **1980**, *48*, 157–173.

(5) Ruedenberg, K.; Schmidt, M. W.; Gilbert, M. M.; Elbert, S. Are atoms intrinsic to

molecular electronic wavefunctions? I. The FORS model. *Chem. Phys.* **1982**, *71*, 41–49.

(6) Andersson, K.; Malmqvist, P. A.; Roos, B. O.; Sadlej, A. J.; Wolinski, K. Second-order perturbation theory with a CASSCF reference function. *J. Phys. Chem.* **1990**, *94*, 5483–5488.

(7) Andersson, K.; Malmqvist, P.-Å.; Roos, B. O. Second-order perturbation theory with a complete active space self-consistent field reference function. *J. Chem. Phys.* **1992**, *96*, 1218–1226.

(8) Andersson, K.; Roos, B. O. Multiconfigurational second-order perturbation theory: A test of geometries and binding energies. *Int. J. Quantum Chem.* **1993**, *45*, 591–607.

(9) Buenker, R. J.; Peyerimhoff, S. D.; Butscher, W. Applicability of the multi-reference double-excitation CI (MRD-CI) method to the calculation of electronic wavefunctions and comparison with related techniques. *Mol. Phys.* **1978**, *35*, 771–791.

(10) Miralles, J.; Castell, O.; Caballol, R.; Malrieu, J.-P. Specific CI calculation of energy differences: Transition energies and bond energies. *Chemical Physics* **1993**, *172*, 33–43.

(11) Calzado, C. J.; Cabrero, J.; Malrieu, J. P.; Caballol, R. Analysis of the magnetic coupling in binuclear complexes. I. Physics of the coupling. *The Journal of Chemical Physics* **2002**, *116*, 2728–2747.

(12) Calzado, C. J.; Cabrero, J.; Malrieu, J. P.; Caballol, R. Analysis of the magnetic coupling in binuclear complexes. II. Derivation of valence effective Hamiltonians from ab initio CI and DFT calculations. *The Journal of Chemical Physics* **2002**, *116*, 3985–4000.

(13) Calzado, C. J.; Angeli, C.; Taratiel, D.; Caballol, R.; Malrieu, J.-P. Analysis of the

magnetic coupling in binuclear systems. III. The role of the ligand to metal charge transfer excitations revisited. *The Journal of Chemical Physics* **2009**, *131*, 044327.

(14) de P. R. Moreira, I.; Suaud, N.; Guihéry, N.; Malrieu, J. P.; Caballol, R.; Bofill, J. M.; Illas, F. Derivation of spin Hamiltonians from the exact Hamiltonian: Application to systems with two unpaired electrons per magnetic site. *Physical Review B* **2002**, *66*, 134430.

(15) Hohenberg, P.; Kohn, W. Inhomogeneous Electron Gas. *Physical Review* **1964**, *136*, B864–B871.

(16) Kohn, W.; Sham, L. J. Self-Consistent Equations Including Exchange and Correlation Effects. *Physical Review* **1965**, *140*, A1133–A1138.

(17) Noodleman, L. Valence bond description of antiferromagnetic coupling in transition metal dimers. *The Journal of Chemical Physics* **1981**, *74*, 5737–5743.

(18) Ginsberg, A. P. Magnetic exchange in transition metal complexes. 12. Calculation of cluster exchange coupling constants with the X.alpha.-scattered wave method. *Journal of the American Chemical Society* **1980**, *102*, 111–117.

(19) Noodleman, L.; Davidson, E. R. Ligand spin polarization and antiferromagnetic coupling in transition metal dimers. *Chemical Physics* **1986**, *109*, 131–143.

(20) Noodleman, L.; Peng, C.; Case, D.; Mouesca, J.-M. Orbital interactions, electron delocalization and spin coupling in iron-sulfur clusters. *Coordination Chemistry Reviews* **1995**, *144*, 199–244.

(21) Bencini, A.; Totti, F.; Daul, C. A.; Doclo, K.; Fantucci, P.; Barone, V. Density Functional Calculations of Magnetic Exchange Interactions in Polynuclear Transition Metal Complexes. *Inorganic Chemistry* **1997**, *36*, 5022–5030.

(22) Ruiz, E.; Cano, J.; Alvarez, S.; Alemany, P. Broken symmetry approach to calculation of exchange coupling constants for homobinuclear and heterobinuclear transition metal complexes. *Journal of Computational Chemistry* **1999**, *20*, 1391–1400.

(23) Yamaguchi, K.; Jensen, F.; Dorigo, A.; Houk, K. A spin correction procedure for unrestricted Hartree-Fock and Møller-Plesset wavefunctions for singlet diradicals and polyradicals. *Chemical Physics Letters* **1988**, *149*, 537–542.

(24) Yamanaka, S.; Okumura, M.; Nakano, M.; Yamaguchi, K. EHF theory of chemical reactions Part 4. UNO CASSCF, UNO CASPT2 and R(U)HF coupled-cluster (CC) wavefunctions. *Journal of Molecular Structure* **1994**, *310*, 205–218.

(25) Yamaguchi, K.; Takahara, Y.; Fueno, T.; Houk, K. N. Extended Hartree-Fock (EHF) theory of chemical reactions. *Theoretica Chimica Acta* **1988**, *73*, 337–364.

(26) Yamaguchi, K.; Fukui, H.; Fueno, T. Molecular orbital (MO) theory for magnetically interacting organic compounds. Ab-initio MO calculations of the effective exchange integrals for cyclophane-type carbene dimers. *Chemistry Letters* **1986**, *15*, 625–628.

(27) Shao, Y.; Head-Gordon, M.; Krylov, A. I. The spin–flip approach within time-dependent density functional theory: Theory and applications to diradicals. *The Journal of Chemical Physics* **2003**, *118*, 4807–4818.

(28) Valero, R.; Illas, F.; Truhlar, D. G. Magnetic Coupling in Transition-Metal Binuclear Complexes by Spin-Flip Time-Dependent Density Functional Theory. *Journal of Chemical Theory and Computation* **2011**, *7*, 3523–3531.

(29) Orms, N.; Krylov, A. I. Singlet–triplet energy gaps and the degree of diradical character in binuclear copper molecular magnets characterized by spin-flip density functional theory. *Physical Chemistry Chemical Physics* **2018**, *20*, 13127–13144.

(30) Seidu, I.; Zhekova, H. R.; Seth, M.; Ziegler, T. Calculation of Exchange Coupling Constants in Triply-Bridged Dinuclear Cu(II) Compounds Based on Spin-Flip Constricted Variational Density Functional Theory. *The Journal of Physical Chemistry A* **2012**, *116*, 2268–2277.

(31) Zhekova, H.; Seth, M.; Ziegler, T. Introduction of a New Theory for the Calculation of Magnetic Coupling Based on Spin–Flip Constricted Variational Density Functional Theory. Application to Trinuclear Copper Complexes which Model the Native Intermediate in Multicopper Oxidases. *Journal of Chemical Theory and Computation* **2011**, *7*, 1858–1866.

(32) Zhekova, H. R.; Seth, M.; Ziegler, T. Calculation of the exchange coupling constants of copper binuclear systems based on spin-flip constricted variational density functional theory. *The Journal of Chemical Physics* **2011**, *135*, 184105.

(33) Peralta, J. E.; Barone, V. Magnetic exchange couplings from noncollinear spin density functional perturbation theory. *The Journal of Chemical Physics* **2008**, *129*, 194107.

(34) Phillips, J. J.; Peralta, J. E. Magnetic Exchange Couplings from Noncollinear Perturbation Theory: Dinuclear CuII Complexes. *The Journal of Physical Chemistry A* **2014**, *118*, 5841–5847.

(35) Filatov, M.; Shaik, S. A spin-restricted ensemble-referenced Kohn–Sham method and its application to diradicaloid situations. *Chemical Physics Letters* **1999**, *304*, 429–437.

(36) Filatov, M. *Density-Functional Methods for Excited States*; Springer International Publishing, 2015; pp 97–124.

(37) Filatov, M.; Huix-Rotllant, M.; Burghardt, I. Ensemble density functional theory method correctly describes bond dissociation, excited state electron transfer, and double excitations. *The Journal of Chemical Physics* **2015**, *142*, 184104.

(38) Filatov, M.; Martínez, T. J.; Kim, K. S. Using the GVB Ansatz to develop ensemble DFT method for describing multiple strongly correlated electron pairs. *Phys. Chem. Chem. Phys.* **2016**, *18*, 21040–21050.

(39) Pérez-Jiménez, Á. J.; Pérez-Jordá, J. M. Combining multiconfigurational wave functions with correlation density functionals: A size-consistent method based on natural orbitals and occupation numbers. *Physical Review A* **2007**, *75*, 012503.

(40) Pérez-Jiménez, Á. J.; Pérez-Jordá, J. M.; de P. R. Moreira, I.; Illas, F. Merging multiconfigurational wavefunctions and correlation functionals to predict magnetic coupling constants. *Journal of Computational Chemistry* **2007**, *28*, 2559–2568.

(41) Sharma, P.; Truhlar, D. G.; Gagliardi, L. Magnetic Coupling in a Tris-hydroxo-Bridged Chromium Dimer Occurs through Ligand Mediated Superexchange in Conjunction with Through-Space Coupling. *Journal of the American Chemical Society* **2020**, *142*, 16644–16650.

(42) Kaduk, B.; Kowalczyk, T.; Voorhis, T. V. Constrained Density Functional Theory. *Chemical Reviews* **2011**, *112*, 321–370.

(43) Rudra, I.; Wu, Q.; Voorhis, T. V. Accurate magnetic exchange couplings in transition-metal complexes from constrained density-functional theory. *The Journal of Chemical Physics* **2006**, *124*, 024103.

(44) Neese, F. Prediction of molecular properties and molecular spectroscopy with density functional theory: From fundamental theory to exchange-coupling. *Coordination Chemistry Reviews* **2009**, *253*, 526–563.

(45) Cramer, C. J.; Truhlar, D. G. Density functional theory for transition metals and transition metal chemistry. *Phys. Chem. Chem. Phys.* **2009**, *11*, 10757–10816.

(46) Loth, P. D.; Cassoux, P.; Daudey, J. P.; Malrieu, J. P. Ab initio direct calculation of the singlet-triplet separation in cupric acetate hydrate dimer. *Journal of the American Chemical Society* **1981**, *103*, 4007–4016.

(47) Coulaud, E.; Guihéry, N.; Malrieu, J.-P.; Hagebaum-Reignier, D.; Siri, D.; Ferré, N. Analysis of the physical contributions to magnetic couplings in broken symmetry density functional theory approach. *The Journal of Chemical Physics* **2012**, *137*, 114106.

(48) Coulaud, E.; Malrieu, J.-P.; Guihéry, N.; Ferré, N. Additive Decomposition of the Physical Components of the Magnetic Coupling from Broken Symmetry Density Functional Theory Calculations. *Journal of Chemical Theory and Computation* **2013**, *9*, 3429–3436.

(49) David, G.; Wennmohs, F.; Neese, F.; Ferré, N. Chemical Tuning of Magnetic Exchange Couplings Using Broken-Symmetry Density Functional Theory. *Inorganic Chemistry* **2018**, *57*, 12769–12776.

(50) Kenny, E. P.; David, G.; Ferré, N.; Jacko, A. C.; Powell, B. J. Frustration, ring exchange, and the absence of long-range order in EtMe3Sb[Pd(dmit)2]2 : From first principles to many-body theory. *Physical Review Materials* **2020**, *4*, 044403.

(51) Trinquier, G.; David, G.; Malrieu, J.-P. Qualitative Views on the Polyradical Character of Long Acenes. *The Journal of Physical Chemistry A* **2018**, *122*, 6926–6933.

(52) David, G.; Trinquier, G.; Malrieu, J.-P. Consistent spin decontamination of broken-symmetry calculations of diradicals. *The Journal of Chemical Physics* **2020**, *153*, 194107.

(53) Ferré, N.; Guihéry, N.; Malrieu, J.-P. Spin decontamination of broken-symmetry density functional theory calculations: deeper insight and new formulations. *Physical Chemistry Chemical Physics* **2015**, *17*, 14375–14382.

(54) David, G.; Ferré, N.; Trinquier, G.; Malrieu, J.-P. Improved evaluation of spin-polarization energy contributions using broken-symmetry calculations. *The Journal of Chemical Physics* **2020**, *153*, 054120.

(55) David, G.; Ferré, N.; Le Guennic, B. Consistent Evaluation of Magnetic Exchange Couplings in Multicenter Compounds in KS-DFT: The Recomposition Method. *Journal of Chemical Theory and Computation* **2022**, *19*, 157–173.

(56) Birkelbach, F.; Winter, M.; Floerke, U.; Haupt, H.-J.; Butzlaff, C.; Lengen, M.; Bill, E.; Trautwein, A. X.; Wieghardt, K.; Chaudhuri, P. Exchange Coupling in Homo- and Heterodinuclear Complexes CuIIM [M = Cr(III), Mn(III), Mn(II), Fe(III), Co(III), Co(II), Ni(II), Cu(II), Zn(II)]. Synthesis, Structures, and Spectroscopic Properties. *Inorganic Chemistry* **1994**, *33*, 3990–4001.

(57) Groom, C. R.; Bruno, I. J.; Lightfoot, M. P.; Ward, S. C. The Cambridge Structural Database. *Acta Crystallographica Section B Structural Science, Crystal Engineering and Materials* **2016**, *72*, 171–179.

(58) Comba, P.; Hausberg, S.; Martin, B. Calculation of Exchange Coupling Constants of Transition Metal Complexes with DFT. *The Journal of Physical Chemistry A* **2009**, *113*, 6751–6755.

(59) Peralta, J. E.; Melo, J. I. Magnetic Exchange Couplings with Range-Separated Hybrid Density Functionals. *J. Chem. Theory Comput.* **2010**, *6*, 1894–1899.

(60) Phillips, J. J.; Peralta, J. E. Magnetic Exchange Couplings from Semilocal Functionals Evaluated Nonself-Consistently on Hybrid Densities: Insights on Relative Importance of Exchange, Correlation, and Delocalization. *Journal of Chemical Theory and Computation* **2012**, *8*, 3147–3158.

(61) Neese, F. The ORCA program system. *Wiley Interdisciplinary Reviews: Computational Molecular Science* **2011**, *2*, 73–78.

(62) Becke, A. D. Density-functional thermochemistry. III. The role of exact exchange. *The Journal of Chemical Physics* **1993**, *98*, 5648–5652.

(63) Lee, C.; Yang, W.; Parr, R. G. Development of the Colle-Salvetti correlation-energy formula into a functional of the electron density. *Physical Review B* **1988**, *37*, 785–789.

(64) Vosko, S. H.; Wilk, L.; Nusair, M. Accurate spin-dependent electron liquid correlation energies for local spin density calculations: a critical analysis. *Canadian Journal of Physics* **1980**, *58*, 1200–1211.

(65) Stephens, P. J.; Devlin, F. J.; Chabalowski, C. F.; Frisch, M. J. Ab Initio Calculation of Vibrational Absorption and Circular Dichroism Spectra Using Density Functional Force Fields. *The Journal of Physical Chemistry* **1994**, *98*, 11623–11627.

(66) Weigend, F.; Ahlrichs, R. Balanced basis sets of split valence, triple zeta valence and quadruple zeta valence quality for H to Rn: Design and assessment of accuracy. *Physical Chemistry Chemical Physics* **2005**, *7*, 3297.

(67) Perdew, J. P.; Burke, K.; Ernzerhof, M. Generalized Gradient Approximation Made Simple. *Physical Review Letters* **1996**, *77*, 3865–3868.

(68) Adamo, C.; Barone, V. Toward reliable density functional methods without adjustable parameters: The PBE0 model. *The Journal of Chemical Physics* **1999**, *110*, 6158–6170.

(69) Ernzerhof, M.; Scuseria, G. E. Assessment of the Perdew–Burke–Ernzerhof exchange-correlation functional. *The Journal of Chemical Physics* **1999**, *110*, 5029–5036.

(70) Moreira, I. d. P. R.; Illas, F.; Martin, R. Effect of Fock exchange on the electronic structure and magnetic coupling in NiO. *Phys. Rev. B* **2002**, *65*, 155102.

(71) Feng, X.; Harrison, N. Magnetic coupling constants from a hybrid density functional with 35% Hartree-Fock exchange. *Phys. Rev. B* **2004**, *70*, 092402.

(72) Assfeld, X.; Rivail, J.-L. Quantum chemical computations on parts of large molecules: the ab initio local self consistent field method. *Chemical Physics Letters* **1996**, *263*, 100–106.

(73) Jmol development team, Jmol. `http://jmol.sourceforge.net/`.

(74) Kahn, O. *Molecular magnetism*; VCH: New York, NY, 1993.